





Synthesis and Biological Evaluation of New Dihydrobenzo[e]indole-Based Schiff Derivatives with Straight and Branched Alkyl Substituents



Wassan Baqir Ali , Salih Mahdi Salman , Mohammed Alwan Farhan , Ekhlas Abdallah Hassan* 

Department of Chemistry, College of Sciences, University of Diyala, Diyala 32001, Iraq

Corresponding Author Email: ekhlasbiochemistry@gmail.com

Copyright: ©2025 The authors. This article is published by IETA and is licensed under the CC BY 4.0 license (<http://creativecommons.org/licenses/by/4.0/>).

<https://doi.org/10.18280/ijdne.200713>

ABSTRACT

Received: 29 June 2025

Revised: 20 July 2025

Accepted: 25 July 2025

Available online: 31 July 2025

Keywords:

Schiff base, benzoindole, tautomer, HepG2, anticancer activity, malonaldehyde

Indoles constitute heterocyclic compounds that have been extensively changed by chemists to produce several variants utilized in various domains of life. This research is an ongoing endeavor that commenced earlier, focusing on the synthesis of benzoindolylene derivatives through the coupling of benzyl amine, aniline, and 4-methyl-o-phenylene diamine out of the Schiff synthesis, with the objective of identifying novel potential anti-cancer medicines. The Schiff reaction occurs among aldehyde and amine groups; therefore, 1,1,2-trimethyl-1H-benzo[e]indole (W1 compound) requires functionalisation to produce two aldehyde groups through treatment with POCl_3 , resulting in 2-(1,1-dimethyl-1H-benzo[e]indol-2(3H)-ylidene) (W2 compound), that can execute the Schiff reaction. The examination of the three-dimensional structure reveals that the proximity of the methyl group to the aldehyde creates steric hindrance, hence prolonging the coupling process with amines from the opposite side. This characteristic enables the regulation of coupling, facilitating the synthesis of mono and di-substituted compounds by reaction of the precursor (W2 Compound) with the specified amines. Five pure chemicals have been synthesized and characterized using spectroscopic methods. The products demonstrate significant efficacy in inhibiting the HepG2 human liver cancer cells at the optimized temperature of 37°C throughout a 24 h period, indicating their potential as cancer treatments. The IC_{50} values for W5 were $58.4 \mu\text{g/ml}$, and for W6 were $46.7 \mu\text{g/ml}$. These findings indicate that compound W6 exhibits higher cytotoxic activity at lower concentrations compared to W5. In conclusion, dihydrobenzindene with both straight and branched aliphatic alkyl attachments can easily achieve a pure state and high yield utilizing (W1) as the precursor by a Schiff reaction following minimal functionalization.

1. INTRODUCTION

Heterocyclic molecules constitute a significant category in organic chemistry, defined as compounds that contain atoms other than Hydrogen and Carbon, including Nitrogen, Oxygen, and Sulfur. There are numerous compounds that include indoles. Benzo indole (W1 compound) represents a significant compound from indoles [1-4]. Numerous alterations are implemented for this substance to identify beneficial applications throughout various domains of life. W1 compound was altered and utilised for the manufacture of fluorescent instruments for in vivo tumour imaging [5-8], Fluorescent instruments sensitive to hypoxia for in vivo acute ischemia, and near-infrared fluorescent instruments for detecting integrin receptor expression [9-11]. W1 is used as an indole pH fluorescent probe and intracellular pH detection and cell marking [12-14]. Another modification of indoles was reported as photodynamic therapy (PDT), the destruction of abnormal cells using a light source and oxygen [15]. The chemical modification of the benzoindole synthon with electrophilic equivalents has resulted in numerous applications for the advancement of near-infrared fluorescence probes [16-

18]. The squaraine dyes derived from the salts of (W1 compound) have been synthesised and used in dye-sensitive solar cells [19, 20]. The dyes of Squaraine, synthesized by using (W1) with various barbituric group combinations attached to the core ring, offer alkyl chains and ester groups on the ring of heterocyclic, especially on nitrogen atoms, demonstrating anti-fungal efficacy versus yeasts. *Saccharomyces cerevisiae* [21]. Treatment for (W1) synthon with acrylic acid derivatives was synthesized and applied for the synthesis of some fluorescent building blocks [22]. 2-(1,1-Dimethyl-1,3-dihydro-benzo[e]indol-2-ylidene)-malonaldehyde is synthesized and reported to show anticonvulsive activity [23]. Another series of benzoindole derivatives shows antimicrobial activity [24]. From the above, the benzoindole derivative (W1 compound) can be logically categorized into: biomedical and pharmaceutical applications, diagnostic and imaging tools, and material science applications.

This survey proves that the benzo indole derivatives applications cover a lot of fields. In continuation with these efforts, this work reports the synthesis of new benzoindole derivatives derived from W1 Compound by coupling with

some aliphatic molecules, including methyl amine and 2-amino butane via Schiff reaction. Several novel compounds demonstrate significant efficacy in inhibiting the HepG2 human cancer of the liver cell lines.

2. MATERIALS AND METHODS

The chemicals, solvents, and reagents utilized in the investigations of this work were procured from various sources and employed. Purification and structural elucidation of the obtained compounds were achieved through ^1H and ^{13}C NMR (Avance Neo 400, Iran), along with IR spectroscopy (Perkin-Elmer) at Diyala University. Chemical structural diagrams and three-dimensional structural analysis were conducted utilizing Chem. Office Ultra 2006 (Cambridge Soft.). The follow-up reactions were conducted by thin layer chromatography (TLC) (dimensions 20.0×20.0 cm) impregnated with silica gel, with detection performed utilizing a Fluorescent Analytical Cabinets Model CM-10. The Stuart SMP10 electronic device is utilized to determine the melting point m.p. of the final compounds.

2.1 General procedure

W1 compound (1 equivalent) was dissolved in 15 ml of dimethylformamide (DMF). Subsequently, a total of 15 ml of phosphorus oxychloride dissolved in DMF was slowly introduced into the initial solution over a duration of thirty minutes at 4°C. The latter was heated at about 90°C for a minimum of 4 h. TLC (6:2) hexane: ethyl acetate indicated the disappearance of W1 from the solution. The completed combination was placed into frozen water and neutralized with 34% NaOH. The products are precipitated, filtered, rinsed with

water, and oven-dried at 55°C to give the W2 compound as yellow crystals [25-28].

2.2 Schiff's reaction

A single equivalent of W2 compound in 15 ml of ethanol was combined with a single equivalent solution of an aliphatic amine in 15 ml of ethanol. Glacial acetic acid (1 cc) was introduced and subjected to reflux. TLC 9:3 hexane: ethyl acetate indicates that the initial material has completely reacted after 14 h. The mono-substituted indole derivatives W3 and W5 precipitate upon solvent removal, undergo filtering, washing, as well as drying. The repetition of the same procedure using compounds W3 and W5 as starting material instead of the W2 compound produced the di-substituted derivatives W4 and W6.

2.3 Synthesis of 2-(1,1-di methyl-1h-benzo[e]indol-2(3h)-ylidene)-3-(methylimino)propanal (W3 compound)

W2 compound (0.2 g, 0.000755 mmol) reacted with methyl amine following the initial coupling technique, resulting in yellow crystals of W3 compound (0.13 g, 0.00047 mmol, 65%), melting point (150°C). ^1H NMR chemical shifts, DMOS as a solvent, at 400 MHz, δ in ppm: δ = 9.79 (s, 0.80H, -CH=O), 9.93 (s, 1H, -CH=N-), 5.52 (s, 0.20H, -C=NH-), 7.36-8.20 (m, 6H, Ar-H), 1.78, 1.94 (s, 6H, 2x CH₃), 1.48 (s, 3H, CH₃). The ^{13}C -NMR spectrum for the synthesized compound W3 displays the following signals (400 MHz, DMSO, δ in ppm): δ = 186.46 (-CH=O), 179.70 for (=CH-OH), 137.90 (-N-C-), 133.03 (-NH-CH=C-), 109.14 (-C=C-), 114.67 (O=C-C=C), 52.93 and 49.33 (CH₃-C-CH₃), 27.16 and 24.45 for 2X CH₃, and 22.59 and 21.55 for CH₃. For more details, see Figures 1 and 2.

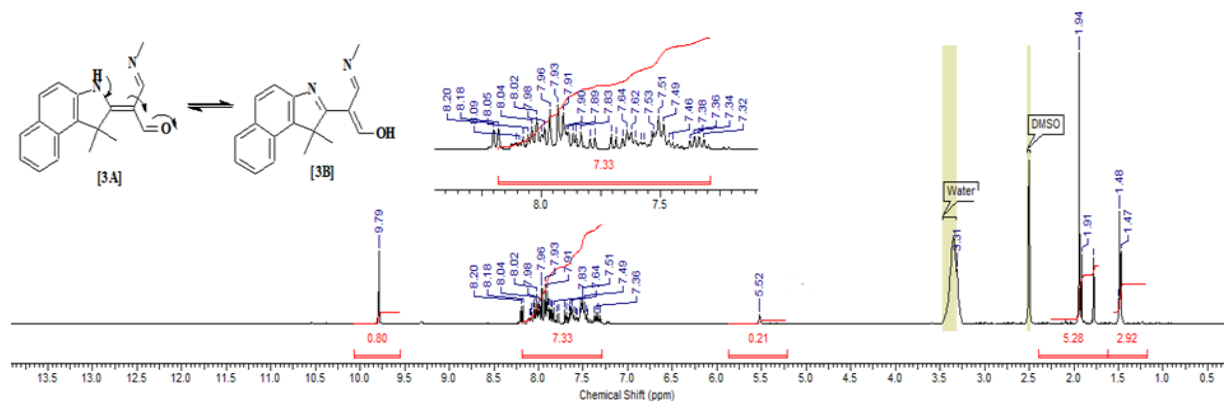


Figure 1. ^1H NMR for W3 compound

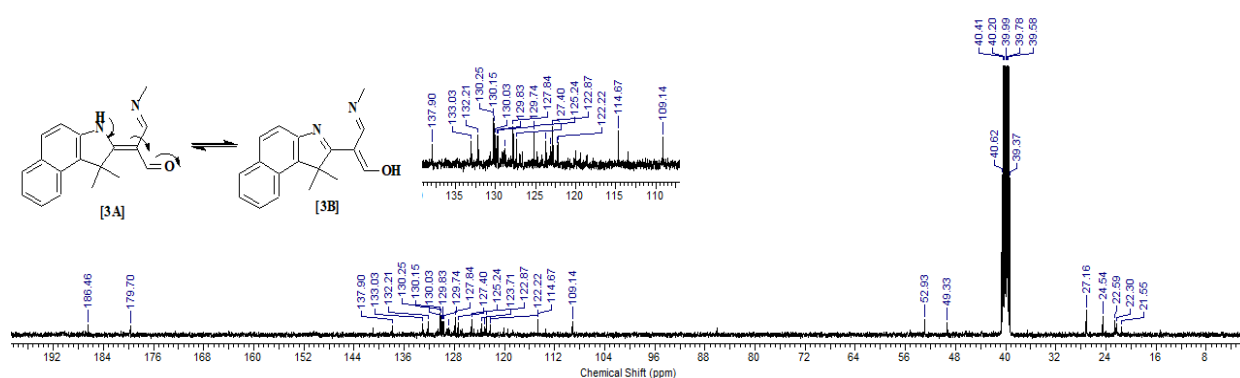


Figure 2. ^{13}C NMR for W3 compound

2.4 Synthesis of 3-(sec-butylimino)-2-(1,1-dimethyl-1h-benzo[e]indol-2(3h)-ylidene)propanal (W5 compound)

W2 Compound (0.2 g, 0.000755 mmole) was subjected to treatment with benzyl amine as previously described in the initial coupling technique, resulting in a brownish-red of W5 Compound (0.18 g, mmole, 64%). With a melting point of 198°C, the compound exhibited the following ^1H NMR

chemical shifts: $\delta = 12.19$ (d, 1H, NH), 9.79 (s, 1H, -CH=O), 7.92 (s, 1H, -CH=N-), 7.48-8.20 (m, 7H, Ar-H), 1.83, 1.93 (s, 6H, 2x CH₃), 1.79 (s, 1H, -N-C*H(CH₃)(CH₂CH₃)), 1.36, 1.08 (d, 3H, CH₃), and 0.98, 0.88 (t, 3H, CH₃). The spectrum of ^{13}C NMR for W5 exhibits the following signals: $\delta = 151.16$ (-N-C-), 139.23 (-NH-CH=C-), 132.12 -N-C= (aromatic), 119.41-129.97 for Ar-C, 30.07 for CH₂, 24.4 and 22.59 for CH₃, and 15.36 for 2XCH₃ (see Figures 3 and 4).

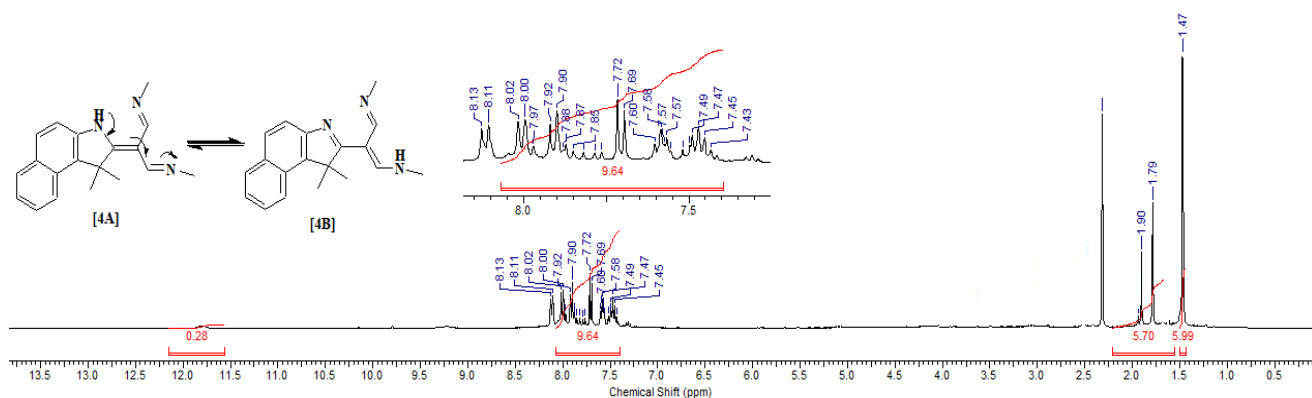


Figure 3. ^1H NMR for W5 compound

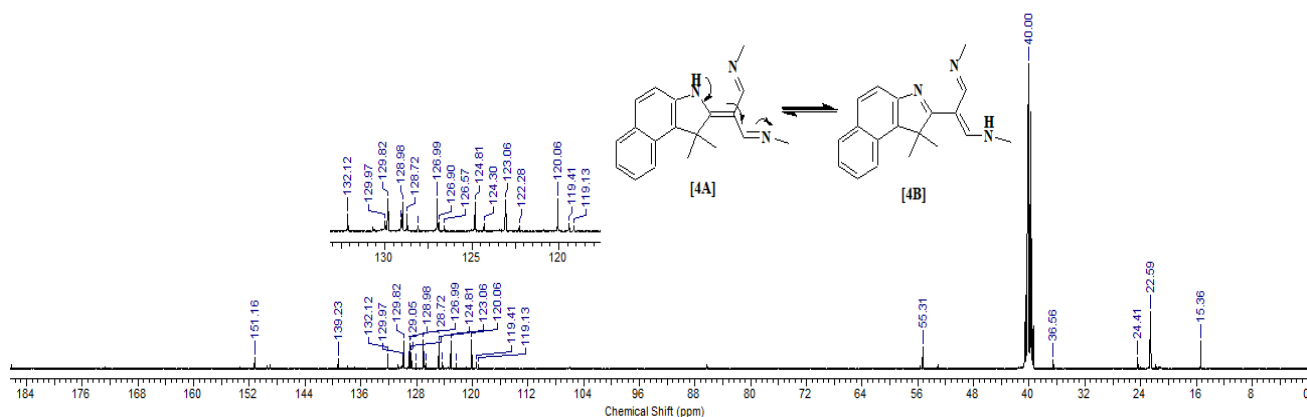


Figure 4. ^{13}C NMR data for compound C5

2.5 Synthesis of 2-(1,1-dimethyl-1h-benzo[e]indol-2(3h)-ylidene)propane-1,3-diylidene dimethanamine (W4 compound)

W2 compound (0.2 g, 0.000590 mmole) reacted with aniline after the initial coupling technique, resulting in brown crystals of W4 compound (0.17 g, mmol, 80%) m.p. 214°C. ^1H NMR expressed in ppm: $\delta = 12.00$ (d, 1H, NH), 7.72 (s, 2H, -CH=N-), 7.43-8.91 (m, 6H, Ar-H), 1.79, 1.90 (s, 6H, 2x CH₃), and 1.47 (s, 6H, 2x CH₃). The spectrum of ^{13}C -NMR for (W4) exhibit the signals: $\delta = 190.25$ for CH=O; 138.41 (NH-CH=C), 109.20 (-C=C-), and 122.86-130.23 (aromatic carbons); 53.00 for -N-C*H(CH₃)(CH₂CH₃); 56.70 for CH₃-C-CH₃; 22.24 for 2XCH₃; 21.16 for CH₃; and 10.37 for CH₃, as shown in Figures 5 and 6.

2.6 Synthesis of 2-(1,1-dimethyl-1h-benzo[e]indol-2(3h)-ylidene)propane-1,3-diylidene)dibutan-2-amine (W6 compound)

W5 compound (0.2 g, 0.00062 mmole) reacted with benzylamine following the initial coupling process, resulting

in a red oily product of W6 compound (0.16 g, mmole, 70%). m.p. 248°C ^1H NMR chemical shifts: $\delta = 12.21$ (d, 1H, NH), 7.69 (s, 1H, -CH=N-), 7.24-8.12 (m, 8H, Ar-H), 1.87, 1.80 (s, 6H, 2x CH₃), 1.69 (s, 2H, -N-C*H(CH₃)(CH₂CH₃)), 1.36, 1.13 (d, 6H, CH₃), 0.98, 0.88 (t, 6H, CH₃). The spectrum of ^{13}C -NMR for W6 exhibits the following signals: $\delta = 137.76$ (-NH-CH=C-), 105.69 (-C=C-), 123.12-129.99 (aromatic carbon), 119.34 (O=C-C=C-), 55.77 for -N-C*H(CH₃)(CH₂CH₃), 56.71 (CH₃-C-CH₃), 30.07 (-CH₂-), 22.38 (2XCH₃), 21.16 for CH₃, and 10.47 for CH₃ (Refer to Figures 7 and 8).

2.7 Anti-cancer activities

The solutions utilized in the present study (RPMI-1640 culture media), following the Giuliano method, solution of Trypsin-Versin, were prepared [29]. The HepG2 cells, as well as normal cell lines (Rhabdomyosarcoma, RD), were cultured in RPMI-1640 media supplemented with 10% foetal calf serum, following the Freshney protocol [30]. The toxicity test was conducted utilizing the crystal violet stain in accordance with Freshney's methodology [31, 32].

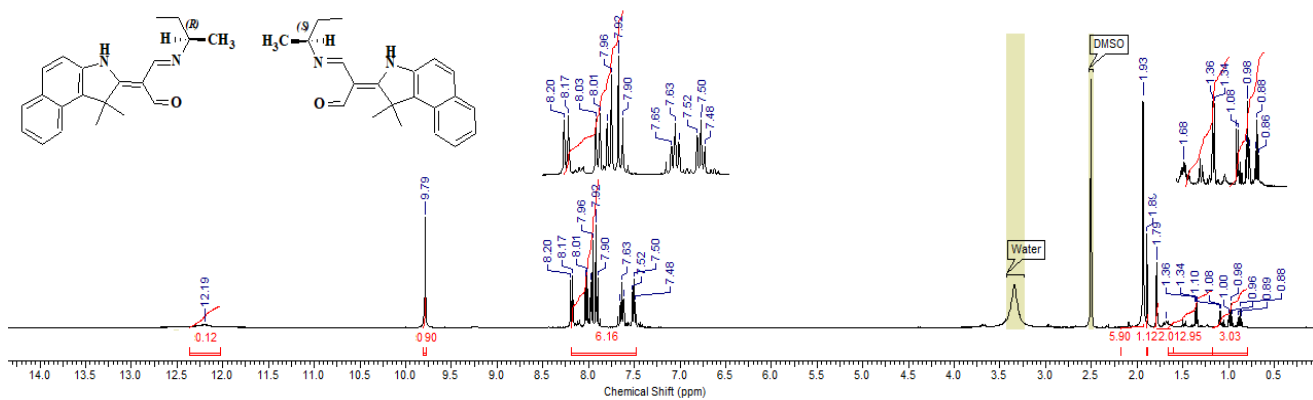


Figure 5. ^1H NMR for W4 compound

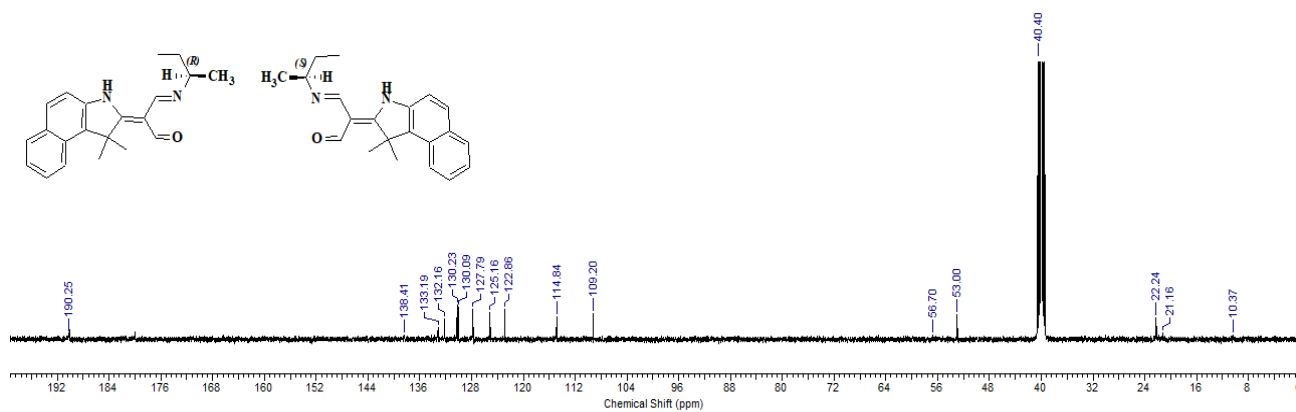


Figure 6. ^{13}C NMR for W4 compound

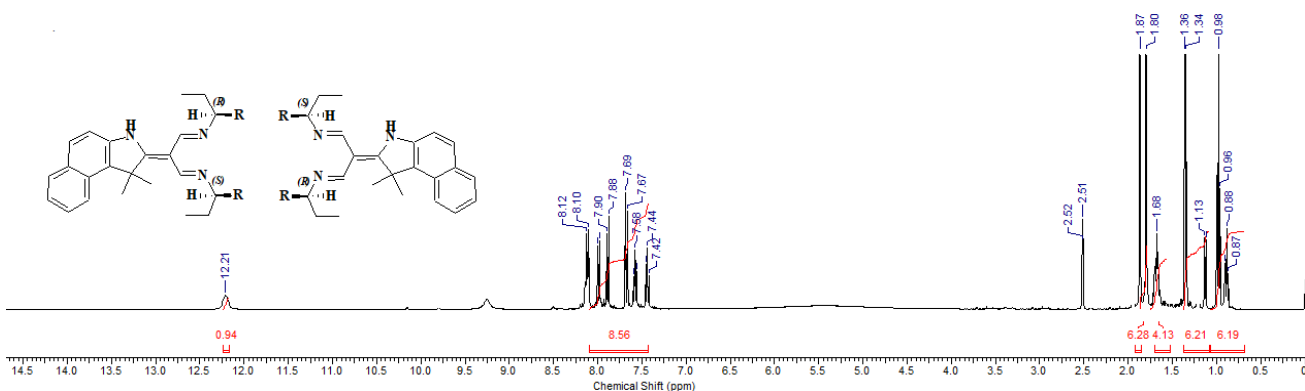


Figure 7. ^1H NMR for W6 compound

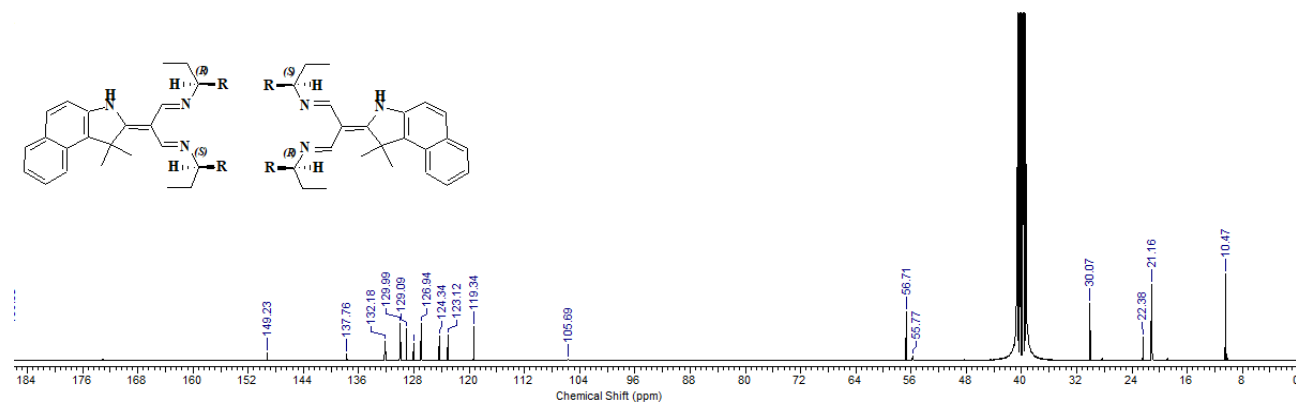


Figure 8. ^{13}C NMR for W6 compound

3. RESULTS AND DISCUSSIONS

3.1 Chemistry

This study seeks to synthesize novel dihydrobenzoylindene compounds and examine their activity. The desired synthesis was accomplished using Schiff's reaction, commencing with (W1) and several aliphatic amines, such as methyl amine and 2-aminobutane, as illustrated in Figure 9.

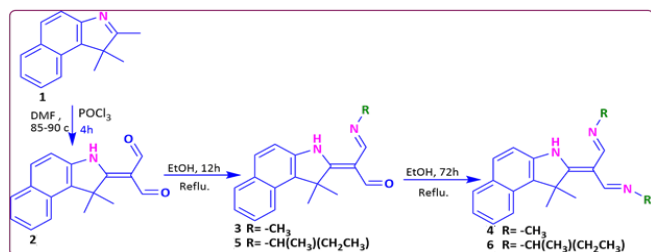


Figure 9. Main synthesis reactions

To facilitate the Schiff's based reaction between W1 and an aliphatic amine, the starting compound requires alteration to introduce an aldehyde group. This may be accomplished by treating the W1 compound with POCl_3 , yielding the previous material, the W2 compound, which contains two groups of aldehyde capable of readily coupling with amino groups in the selected compounds. The reactions of Schiff's bases under moderate circumstances were utilized on the previous material W2 to prepare the di-substituted dihydrobenzindole derivatives with the specified amines. However, this reaction yielded unanticipated mono-substituted derivatives instead of di-substituted dihydrobenzindole, despite the application of one equivalent of precursor with two equivalents of amine. Consequently, the reactions of the W2 compound with methyl amine and 4-methyl-2-aminobutane yielded the mono-substituted dihydrobenzindolylidene W3 and W5 compounds in place of the di-substituted derivatives W4 and W6. Three-dimensional studies of the reactive intermediate indicate that the formation of mono-substituted derivatives, rather than disubstituted ones, during short reaction periods, is attributed to steric hindrance near the reaction center caused by the presence of methyl groups on the indole ring. But the di-substituted derivatives need a longer reaction time after the first coupling. So the first 12 h of the reaction, the mono-substituted derivatives are separated as NMR pure crystals, while the di-substituted derivatives are achieved when the reaction is carried out for 72 h, using the mono-derivatives as starting materials with the same amines. The mono-derivatives are characterized by ^1H NMR spectroscopy, for W3 the NH proton of the indole appears at about 13.0 ppm, the aldehyde protons exist at 9.79 ppm, $-\text{CH}=\text{N}-$ appears around 9.5 ppm, aromatics protons shown at about 7.50 to 8.00 ppm, proton of $-\text{CH}-\text{NH}$ (tautomer) at about 7.26 and the six protons of the methyl groups of indole appears at about 1.8-1.95 ppm in addition to CH_3 protons of the aliphatic moiety appear at about 1.48. The ^{13}C -NMR spectra for W3 show the signals of $-\text{CH}=\text{O}$ at $\delta = 186.46, 137.90$ for $\text{N}-\text{C}$, 133.03 ($-\text{NH}-\text{CH}=\text{C}-$), 109.14 for $-\text{C}=\text{C}-$, 122.22- 130.25 (aromatic carbons), 114.67 ($\text{O}=\text{C}-\text{C}=\text{C}-$), 52.93 and 49.33 ($\text{CH}_3-\text{C}-\text{CH}_3$), 27.16, 24.45 for 2XCH_3 and 22.59, 21.55 for CH_3 , see Figure 1 for ^1H and Figure 2 for ^{13}C NMR analyses for more details. The same chemical shift appears for compound W5 in both ^1H and ^{13}C NMR, in addition to the peaks of the alkyl moiety at 52.77 for

$-\text{N}-\text{C}^*\text{H}(\text{CH}_3)(\text{CH}_2\text{CH}_3)$, 30.07 for CH_2 and 21.16 for CH_3 and 10.347 for CH_3 ppm for both aliphatic terminal methyl, see Figure 3 for ^1H and Figure 4 for ^{13}C NMR analyses for more details. The di-substituted synthesized compound derivatives W4 and W6 show the same chemical shift as the mono-substituted derivatives with multiple integration protons and carbons (see Figures 5-8). The appearance of double peaks for each proton in NMR analysis confirms that compounds 3 and 5 show a tautomeric state for example the appearance of two peaks with one integration at 9.79 with 0.80 integration and 5.50 with 0.20 prove the tautomeric state of W3 which is appear as two tautomer 3A 80% and 3B 20% as the proton in 3A stabilized by hydrogen bonding with imine nitrogen (Figure 10).

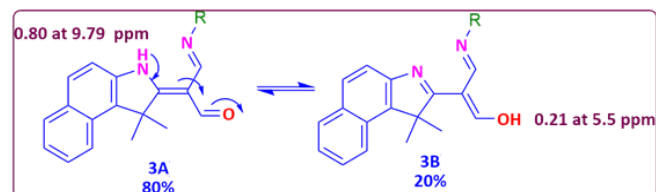


Figure 10. Tautomerism of the W3 compound

The two di-substituted compounds contain chiral carbon, so that they have two enantiomers (R) and (S), they show double peaks, one for each proton, with approximately the same tensions as they are a racemic mixture (Figure 11).

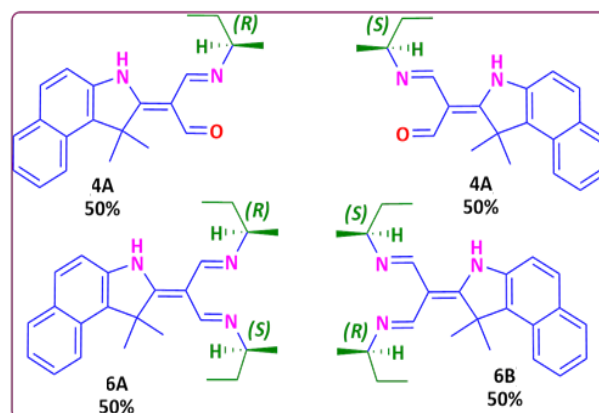


Figure 11. Stereoisomers of compounds W4 and W6

3.2 Anti-cancer activities

The anticancer activity of the two synthesized compounds was evaluated using the cancer cell line, as presented in Table 1. The examined compounds exhibit significant activity in inhibiting HepG2 under the optimal temperature condition of 37°C , over a 24h period, utilizing two doses (50 $\mu\text{g}/\text{ml}$ and 100 $\mu\text{g}/\text{ml}$), in contrast to their effects on a normal cell line. The derivative of dihydrobenzindene with W5 exhibits more activity in high concentration solutions (50 $\mu\text{g}/\text{ml}$) compared to the branching derivatives; however, in low concentration solutions, the di-substituted analogue of the identical compounds W4 and W6 is more effective. W6 compound has enhanced anticancer activity compared to the linear counterpart. As a result, both examined compounds showed a significant capability to inhibit the HepG2 cancer cell line, rendering them acceptable for medical application as anticancer medicines.

The percentage of cell inhibition was calculated based on the crystal violet assay. For compound W5, the inhibition rates were 31.21% and 53.19% at 50 and 100 µg/ml, respectively. For compound W6, the inhibition rates were 48.24% and 66.10%, respectively. Based on the obtained data, the IC₅₀ values were estimated using non-linear regression analysis with GraphPad Prism software. The IC₅₀ values for W5 and W6 were calculated as: W5: IC₅₀ = 58.4 µg/ml, W6: IC₅₀ = 46.7 µg/ml. These findings indicate that compound W6 exhibits higher cytotoxic activity at lower concentrations compared to W5.

Table 1. The impact of certain synthesized derivatives on cancerous and normal cell lines

Com. No.	Inhibition Conc. for Normal Cell Line RD (µg/ml)		Inhibition Conc. for Cell Line Cancer HepG2 (µg/ml)	
	50	100	50	100
W5	31.21	53.19	40.70	57.85
W6	48.24	66.10	40.70	18.20

3.3 The suggestion mechanism for anticancer of Schiff base derivatives

Schiff base derivatives are well-recognized for their biological activity, including anticancer properties. The anticancer mechanism of these compounds is believed to involve multiple pathways. One prominent mechanism is the interaction with DNA [33, 34]. Another key pathway involves the generation of reactive oxygen species (ROS), which induces oxidative stress, leading to mitochondrial dysfunction and subsequent apoptosis (programmed cell death). Additionally, Schiff base derivatives have been shown to interfere with the activity of key enzymes involved in cancer cell survival, such as topoisomerases and kinases [35]. In the present study, the observed inhibition of HepG2 liver cancer cells suggests that the synthesized Schiff base derivatives may act through one or more of these mechanisms. The structural presence of electron-donating groups (e.g., alkyl chains and imine linkages) may enhance lipophilicity, facilitating membrane permeability and intracellular accumulation, which further supports their cytotoxic action.

3.4 Limitations and future directions

While the current study demonstrates the promising anticancer potential of newly synthesized dihydrobenzindolylidene Schiff base derivatives against HepG2 liver cancer cells, it is not without limitations. Notably, the biological evaluation was limited to *in vitro* cytotoxicity assays, and no *in vivo* studies or animal models were conducted to confirm the compounds' efficacy, bioavailability, toxicity, or pharmacokinetic behavior. Additionally, the molecular mechanism underlying the observed anticancer activity was not directly investigated and remains speculative. The future research should focus on:

- Conducting *in vivo* studies using animal models to validate the anticancer efficacy and assess systemic toxicity.
- Performing mechanistic studies, such as apoptosis assays, ROS generation, and cell cycle analysis, to elucidate how these compounds induce cell death.
- Evaluating the structure-activity relationship (SAR) by synthesizing analogues with varied substituents.

- Exploring targeted delivery systems or nanocarrier formulations to improve bioavailability and selectivity of these Schiff base derivatives.

4. CONCLUSION

In conclusion, dihydrobenzoin-dolylidene with both straight and branched aliphatic alkyl attachments can easily achieve a pure state and high yield utilizing W1 as the precursor by a Schiff reaction following minimal functionalization. This series demonstrates significant action against the HepG2 human cancer of the liver cell lines, exhibiting inhibition at the optimized temperature of 37°C during a 24 h period with varying doses. This feature renders the target chemicals as anticancer agents.

ACKNOWLEDGMENT

Researchers express their gratitude to the University of Diyala, College of Sciences, for supplying the necessary resources to conduct the study.

REFERENCES

- [1] Sathya, V., Deepa, A., Sangeetha, L.K., Srinivasadesikan, V., Lee, S.L., Padmini, V. (2022). Development of optical biosensor for the detection of glutamine in human biofluids using merocyanine dye. *Journal of Fluorescence*, 32(4): 1389-1396. <https://doi.org/10.1007/s10895-022-02937-y>
- [2] Menéndez, G.O., Pichel, M.E., Spagnuolo, C.C., Jares-Erijman, E.A. (2013). NIR fluorescent biotinylated cyanine dye: Optical properties and combination with quantum dots as a potential sensing device. *Photochemical & Photobiological Sciences*, 12(2): 236-240. <https://doi.org/10.1039/c2pp25174d>
- [3] Zhang, K., Meng, J., Bao, W., Liu, M., Wang, X., Tian, Z. (2021). Mitochondrion-targeting near-infrared fluorescent probe for detecting intracellular nanomolar level hydrogen sulfide with high recognition rate. *Analytical and Bioanalytical Chemistry*, 413(4): 1215-1224. <https://doi.org/10.1007/s00216-020-03086-6>
- [4] Miki, K., Kimura, A., Oride, K., Kuramochi, Y., Matsuoka, H., Harada, H., Ohe, K. (2011). High-contrast fluorescence imaging of tumors *in vivo* using nanoparticles of amphiphilic brush-like copolymers produced by ROMP. *Angewandte Chemie International Edition*, 50(29): 6567-6570. <https://doi.org/10.1002/anie.201101005>
- [5] Onoe, S., Temma, T., Kanazaki, K., Ono, M., Saji, H. (2015). Development of photostabilized asymmetrical cyanine dyes for *in vivo* photoacoustic imaging of tumors. *Journal of Biomedical Optics*, 20(9): 096006. <https://doi.org/10.1117/1.JBO.20.9.096006>
- [6] Farhan, M.A., Al-Garawi, Z.S., Ali, W.B., Nief, O.A. (2023). A novel method for long-term preserving of urine microstructure using poly (vinyl chloride). *Journal of Applied Polymer Science*, 140(26): 54000. <https://doi.org/10.1002/app.54000>
- [7] Farhana, M.A., Nief, O.A., Alib, W.B. (2022). New photostabilizers for poly (vinyl chloride) derived from

- heterocyclic compounds. *Eurasian Chemical Communications*, 4(6): 525-543. <https://doi.org/10.22034/ecc.2022.332467.1347>
- [8] Mohammed, L.A., Farhan, M.A., Dadoosh, S.A., Alheety, M.A., Majeed, A.H., Mahmood, A.S., Mahmoud, Z.H. (2023). A review on benzimidazole heterocyclic compounds: Synthesis and their medicinal activity applications. *SynOpen*, 7(4): 652-673. <https://doi.org/10.1055/a-2155-9125>
- [9] Li, S.J., Zhou, D.Y., Li, Y.F., Yang, B., Ou-Yang, J., Jie, J., Li, C.Y. (2018). Mitochondria-targeted near-infrared fluorescent probe for the detection of carbon monoxide in vivo. *Talanta*, 188: 691-700. <https://doi.org/10.1016/j.talanta.2018.06.046>
- [10] Kiyose, K., Hanaoka, K., Oushiki, D., Nakamura, T., Kajimura, M., Suematsu, M., Nagano, T. (2010). Hypoxia-sensitive fluorescent probes for in vivo real-time fluorescence imaging of acute ischemia. *Journal of the American Chemical Society*, 132(45): 15846-15848. <https://doi.org/10.1021/ja105937q>
- [11] Wang, H., Wang, X., Li, P., Dong, M., Yao, S.Q., Tang, B. (2021). Fluorescent probes for visualizing ROS-associated proteins in disease. *Chemical Science*, 12(35): 11620-11646. <https://doi.org/10.1039/D1SC02165F>
- [12] Niu, W., Nan, M., Fan, L., Wong, M.S., Shuang, S., Dong, C. (2016). A novel pH fluorescent probe based on indocyanine for imaging of living cells. *Dyes and Pigments*, 126: 224-231. <https://doi.org/10.1016/j.dyepig.2015.11.027>
- [13] Liu, X.D., Xu, Y., Sun, R., Xu, Y.J., Lu, J.M., Ge, J.F. (2013). A coumarin-indole-based near-infrared ratiometric pH probe for intracellular fluorescence imaging. *Analyst*, 138(21): 6542-6550. <https://doi.org/10.1039/C3AN01033C>
- [14] Wen, Y., Jing, N., Huo, F., Yin, C. (2021). Recent progress of organic small molecule-based fluorescent probes for intracellular pH sensing. *Analyst*, 146(24): 7450-7463. <https://doi.org/10.1039/D1AN01621K>
- [15] Varvuolytė, G., Malina, L., Bieliauskas, A., Hošíková, B., Simerska, H., Kolářová, H., Žukauskaitė, A. (2020). Synthesis and photodynamic properties of pyrazole-indole hybrids in the human skin melanoma cell line G361. *Dyes and Pigments*, 183: 108666. <https://doi.org/10.1016/j.dyepig.2020.108666>
- [16] Sun, C.L., Lv, S.K., Liu, Y.P., Liao, Q., Zhang, H.L., Fu, H., Yao, J. (2017). Benzoinidolic squaraine dyes with a large two-photon absorption cross-section. *Journal of Materials Chemistry C*, 5(5): 1224-1230. <https://doi.org/10.1039/C6TC04129A>
- [17] Gong, X., Yang, X.F., Zhong, Y., Chen, Y., Li, Z. (2016). A mitochondria-targetable near-infrared fluorescent probe for imaging nitroxyl (HNO) in living cells. *Dyes and Pigments*, 131: 24-32. <https://doi.org/10.1016/j.dyepig.2016.03.046>
- [18] Han, C., Yang, H., Chen, M., Su, Q., Feng, W., Li, F. (2015). Mitochondria-targeted near-infrared fluorescent off-on probe for selective detection of cysteine in living cells and in vivo. *ACS Applied Materials & Interfaces*, 7(50): 27968-27975. <https://doi.org/10.1021/acsami.5b10607>
- [19] Connell, A., Holliman, P.J., Davies, M.L., Gwenin, C.D., Weiss, S., Pitak, M.B., Cooke, G. (2014). A study of dye anchoring points in half-squarylium dyes for dye-sensitized solar cells. *Journal of Materials Chemistry A*, 2(11): 4055-4066. <https://doi.org/10.1039/C3TA15278B>
- [20] Khopkar, S., Jachak, M., Shankarling, G. (2019). Viscosity sensitive semisquaraines based on 1, 1, 2-trimethyl-1H-benzo[e]indole: Photophysical properties, intramolecular charge transfer, solvatochromism, electrochemical and DFT study. *Journal of Molecular Liquids*, 285: 123-135. <https://doi.org/10.1016/j.molliq.2019.03.173>
- [21] Gomes, V.S., Ferreira, J.C., Boto, R.E., Almeida, P., Fernandes, J.R., Sousa, M.J., Reis, L.V. (2022). Squaraine dyes derived from indolenine and benzo [e] indole as potential fluorescent probes for HSA detection and antifungal agents. *Photochemistry and Photobiology*, 98(6): 1402-1417. <https://doi.org/10.1111/php.13624>
- [22] Steponavičiūtė, R., Martynaitis, V., Bieliauskas, A., Šačkus, A. (2014). Synthesis of new fluorescent building blocks via the microwave-assisted annulation reaction of 1, 1, 2-trimethyl-1H-benzo [e] indole with acrylic acid and its derivatives. *Tetrahedron*, 70(11): 1967-1974. <https://doi.org/10.1016/j.tet.2014.01.070>
- [23] Rothan, H.A., Amini, E., Faraj, F.L., Golpich, M., Teoh, T.C., Gholami, K., Yusof, R. (2017). NMDA receptor antagonism with novel indolyl, 2-(1, 1-Dimethyl-1, 3-dihydro-benzo [e] indol-2-ylidene)-malonaldehyde, reduces seizures duration in a rat model of epilepsy. *Scientific Reports*, 7(1): 45540. <https://doi.org/10.1038/srep45540>
- [24] Simakov, S., Kartsev, V., Petrou, A., Nicolaou, I., Geronikaki, A., Ivanov, M., Vizirianakis, I.S. (2021). 4-(Indol-3-yl) thiazole-2-amines and 4-undol-3-yl) thiazole acylamines as novel antimicrobial agents: Synthesis, in silico and in vitro evaluation. *Pharmaceuticals*, 14(11): 1096. <https://doi.org/10.3390/ph14111096>
- [25] Salih, S.M., Alkubaisi, H.M., Faraj, F.L. (2021). Synthesis and characterization of novel pyrazole derivatives from 4-florophenylhydrazine and study their cytotoxicity as anti-cancer agent. *Egyptian Journal of Chemistry*, 64(11): 6473-6480. <https://doi.org/10.21608/ejchem.2021.78214.3825>
- [26] Mekheimer, R.A., Al-Sheikh, M.A., Medrasi, H.Y., Sadek, K.U. (2020). Advancements in the synthesis of fused tetracyclic quinoline derivatives. *RSC Advances*, 10(34): 19867-19935. <https://doi.org/10.1039/D0RA02786C>
- [27] Essam, Z.M., Ozmen, G.E., Setiawan, D., Hamid, R.R., Abd El-Aal, R.M., Aneja, R., Henary, M. (2021). Donor acceptor fluorophores: Synthesis, optical properties, TD-DFT and cytotoxicity studies. *Organic & Biomolecular Chemistry*, 19(8): 1835-1846. <https://doi.org/10.1039/D0OB02313B>
- [28] Farhan, M.A., Ali, W.B., Ibrahim, W.A., Mahmoud, Z.H. (2024). Anti-cancer Schiff bases as photostabilizer for poly (vinyl chloride). *Bulletin of the Chemical Society of Ethiopia*, 38(1): 135-146. <https://dx.doi.org/10.4314/bcse.v38i1.11>
- [29] Calvaruso, G., Giuliano, M., Portanova, P., Pellerito, O., Vento, R., Tesoriere, G. (2007). Hsp72 controls bortezomib-induced HepG2 cell death via interaction with pro-apoptotic factors. *Oncology Reports*, 18(2): 447-450. <https://doi.org/10.3892/or.18.2.447>
- [30] Rahman, H., Qasim, M., Schultze, F.C., Oellerich, M., Asif, A.R. (2011). Fetal calf serum heat inactivation and lipopolysaccharide contamination influence the human T lymphoblast proteome and phosphoproteome. *Proteome*

- Science, 9(1): 71. <https://doi.org/10.1186/1477-5956-9-71>
- [31] Vibin, M., Vinayakan, R., John, A., Raji, V., Rejiya, C.S., Vinesh, N.S., Abraham, A. (2011). Cytotoxicity and fluorescence studies of silica-coated CdSe quantum dots for bioimaging applications. *Journal of Nanoparticle Research*, 13(6): 2587-2596. <https://doi.org/10.1007/s11051-010-0151-8>
- [32] Farhan, M.A., Ibrahim, W.A., Ali, W.B. (2023). Synthesis, evaluation of anticancer and antimicrobial activities of some Schiff bases derivatives. *Al-Kitab Journal for Pure Sciences*, 7(2): 115-129. <https://doi.org/10.32441/kjps.07.02.p10>
- [33] Ajaj, Y., Mahmoud, Z.H., Obeed, A.N., Al-Salih, M., Ahmed, B.A., Hassan, E.A., Kianfar, E. (2024). Molecular motors in nanobiotechnology: Protein and DNA based molecular motors: A review. *Results in Chemistry*, 7: 101250. <https://doi.org/10.1016/j.rechem.2023.101250>
- [34] Al-Azzawi, A.M., Hassan, E.A. (2025). Exploring benzo [d] thiazol-2-amine derivatives, synthesis, and molecular docking insights potential anticancer agents targeting HER Enzyme and DNA. *Applied Biochemistry and Biotechnology*, 197(4): 2383-2396. <https://doi.org/10.1007/s12010-024-05149-1>
- [35] Hajrezaie, M., Paydar, M., Zorofchian Moghadamtousi, S., Hassandarvish, P., Gwaram, N.S., Zahedifard, M., Abdulla, M.A. (2014). A Schiff base-derived copper (II) complex is a potent inducer of apoptosis in colon cancer cells by activating the intrinsic pathway. *The Scientific World Journal*, 2014(1): 540463. <http://doi.org/10.1155/2014/540463>